Selective solar absorbers: A cost effective solution for access to clean energy in rural Africa

G KATUMBA*, L OLUMEKOR†, A FORBES*
*CSIR National Laser Centre, PO Box 395, Pretoria, 0001, South Africa
†Physics Department, University of Zimbabwe, P O Box MP 167, Mt. Pleasant, Harare, Zimbabwe
Email: gkatumba@csir.co.za

Abstract
In this present era of global energy crisis there is a greater need to turn to renewable, cost effective and sustainable energy resources. In rural Africa, in particular, the demand for domestic energy is even higher. This is exacerbated by inadequate grid electricity infrastructure. This state of affairs has culminated in massive deforestation and desertification of some parts of Africa. One technology solution is to harness the energy from the sun through solar absorbers. This has applications in domestic heating – such as heating water (solar geysers) and cooking food. Early solar energy technologies were not readily accepted in Africa because of high initial investment cost and low efficiency, particularly so for the less affluent rural populace. Presently, there is a re–look into the solar energy technologies with emphasis on cost effectiveness and sustainability.

In this paper we present new results on a novel selective solar absorber material. Laboratory tests show that it is about 30% more efficient than the best alternative on the market. Our novel selective solar absorber material comprises carbon nanoparticles embedded in a NiO matrix on an aluminium substrate. It shows enhanced solar radiation absorptance and low thermal emittance properties. The sol-gel recipe that is used to manufacture the material has additional advantages of being environmentally friendly and of having a low production cost. We report on a planned prototype development programme to take the laboratory solution into the field, and highlight the likely impact this will have on rural communities. The low cost aspect of this novel solution makes it particularly suitable for the African continent.

1. Introduction

The search for low cost and efficient spectrally selective solar absorber materials continues unabated. There is a large volume of literature indicating the activities in the field of selective solar absorber materials (Katumba, 2008a; Katumba 2008b; Katumba 2008c, Avila-Garcia, 2006; Zhao, 2006; Katumba 2005; Konttinen, 2003; Orel, 1999; Niklasson, 1984). Some of the research work has resulted in commercial products that are currently on the market (Orel, 1999).

The manufacturing processes for most of the commercially available solar thermal products require complicated and expensive equipments. Some have high input material consumption. The requirements of selective solar absorber materials used for low to moderate temperature applications such as domestic water heating collectors are:

- High absorption in the solar wavelength range
- Low thermal emittance in the near-infrared (NIR) and far-infrared (FIR) wavelength ranges.

These requirements translate to a material that has low reflectance (less than 10%) in the wavelength range from 0.3 to 2.5 μm and a high reflectance (larger than 90%) for wavelengths longer than 2.5 μm. Today, no intrinsic material is capable of this selectivity. There is therefore a need to be able to tailor the optical and structural properties of a material or a combination of materials to achieve the desired wavelength selectivity. One technique is to make thin solar absorbing coatings on suitably reflecting metallic substrates. Control of the spectral selectivity in the coating is achieved by adjusting various parameters of the coatings such as composition, thickness, porosity, surface morphology and nanostructure, among others.

In this work, the spectral selectivity of composite coatings of carbon nanoparticles dispersed in each of two different dielectric matrices of ZnO and NiO is compared as a function of the ratio of solar absorptance to thermal emittance. Some structural analysis of the samples is made to understand the optical and thermal behaviour of the coatings. The

selective solar absorber systems reported here have had no reported investigation previously.

2. Theoretical considerations

The concept of a spectrally selective solar-absorbing surface can best be described by the illustration in Fig. 1. There is minimal overlap between the solar spectral range of air mass (AM) 1.5 and the thermal emittance spectra at three temperatures of a blackbody-like surface. The non-overlap between the solar radiation and emittance spectra provides an opportunity to tailor a material or a combination of materials to achieve spectral selectivity that is close to an ideal absorber, the spectral reflectance of which is shown as the step function in Fig. 1. The step change from low to high reflectance should be at a wavelength of between 2.0 and 3.0 μm for an effective solar heating application at temperatures below 400 ℃.

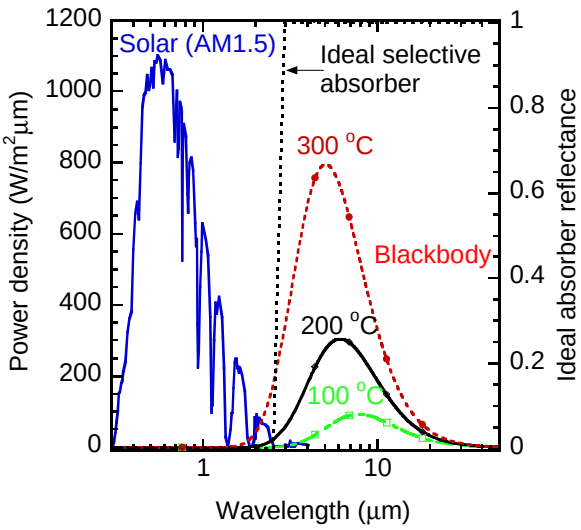

Fig. 1: An annotation showing minimal overlap between the sun spectrum at AM 1.5 (ISO standard 9845–1 (1992)) and the blackbody-like emission spectra at 100 °C, 200 °C and 300 °C. A reflectance curve for an ideal selective solar absorber is included.

The solar absorptance α of a solar collector surface is defined as fraction of radiation incident on the surface of the material that is absorbed. It is a function of both the incident spectrum, $I_{sol}(\lambda)$, and the reflection function of the material, R (λ), and is given by:

$$\alpha = \frac{\int_{0.3\mu m}^{2.5\mu m} I_{sol}(\lambda)(1-R(\lambda))d\lambda}{\int_{0.3\mu m}^{2.5\mu m} I_{sol}(\lambda)d\lambda}$$

Likewise, the fractional emittance may be defined as the weighted fraction (by total power density) of the emitted radiation:

$$\varepsilon = \frac{\int_{2.5\mu m}^{20\mu m} \rho(\lambda)(1-R(\lambda))d\lambda}{\int_{2.5\mu m}^{20\mu m} \rho(\lambda)d\lambda}$$

where $\rho(\lambda)$ is the blackbody spectrum. It is usual practice to compare the selectivities of different surfaces by comparing the ratio of solar absorptance to thermal emittance:

$$\xi = \frac{\alpha}{\varepsilon}$$

The notion of this comparison is simply that the larger the value of ξ, the better the selectivity.

Many selective solar absorber designs are possible (Wäckelgård, 2001) but here discussion is centred on a composite coating on a metallic substrate of adequate infrared reflectance. This tandem device is illustrated in Fig. 2. The composite layer comprises carbon nanoparticles dispersed in either of the ZnO or NiO dielectric matrix.

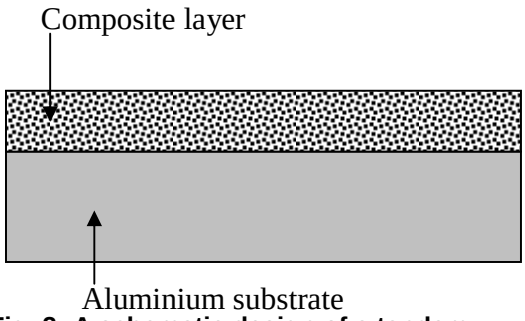

Fig. 2: A schematic design of a tandem selective solar absorber in a cross sectional view consisting of highly absorbing composite coating on highly reflecting aluminium.

3. Experimental setup and measurements

3.1. Substrate preparation

The C-ZnO and C-NiO samples were prepared on rolled aluminium substrates. The substrate preparation of the samples was adopted from a previous experiment (Katumba, 2005).

3.2 Sample preparation

A novel sol-gel technique closely related to the method of Liu *et al*. (Liu, 2005) has been used to prepare both the ZnO and NiO samples. Appropriate quantities of zinc acetate [($ZnAc_2$), $Zn(CH_3COO)_2.2H_2O$] and nickel acetate [($NiAc_2$), $Ni(CH_3COO)_2.4H_2O$] were separately dissolved in 50 ml of absolute ethanol [(EtOH), CH_3CH_2OH,] by magnetic stirring at room temperature. An amount of diethanolamine [(DEA), $NH(CH_2CH_2OH)_2$] was added as chelating agent such that the molar ratio of each acetate type to DEA and to SUC was also maintained at 1:1:0.6. These solutions formed the ZnO and NiO precursors. The SUC was dissolved in doubly distilled and deionised water in the mass ratio 1:1 prior to mixing with the matrix precursor solutions. This constituted the carbon precursor solution. The oxide and carbon precursor solutions were mixed and stirred again. After a period of stirring 1 g of polyethylene glycol [(PEG), $HO(CH_2CH_2O)_nH$] was added to the ZnO and NiO matrix precursor sols. The resultant solution was further stirred until the formation of a sol that was immediately spin-coated onto pre-cleaned aluminium substrates. The PEG was used as a structure directing template. The spin-coated samples were calcined in a tube furnace in flowing nitrogen gas at 550 °C for one hour to carbonise the carbon precursor and to also dry and densify the oxide matrix. This method ensured an even distribution of the carbon nanoparticles in the oxide matrices.

3.2. Optical measurements

The near-normal spectral reflectance of the samples was measured in the 0.3 to 2.5 μm wavelength range with a Perkin Elmer Lambda 900 spectrophotometer. A spectralon sample was used for reference spectrum measurements. A Bomem DA8 Fourier Transform spectrometer was used to measure near-normal reflectance in the 2.5 to 20.0 μm wavelength range. A mercury cadmium telluride detector cooled in liquid nitrogen was used for these infrared (IR) measurements. The IR measurements were corroborated with measurements on a Bruker Tensor 27 spectrophotometer with a gold mirror reference. The reflectance measurements were used to calculate solar absorptance, α and thermal emittance, ε of the samples at 100 ℃.

3.3. Non-optical measurements

The surface morphology of all samples was studied with a Philips XL30 scanning electron microscope (SEM). The cross-sectional fine structure of the samples was investigated with a Tecnai F30 ST high resolution transmission electron microscopy (X-HRTEM). Energy dispersive spectroscopy (EDS) and electron energy loss spectroscopy (EELS) studies were performed with the Tecnai F30 microscope. The crystal structure of the C-ZnO and C-NiO samples was investigated with a Philips PW 1840 diffractometer using a CuK_α target at 35 keV and 30 mA.

4. Results and discussion

4.1 SEM results

The SEM representative images of the C-ZnO and C-NiO samples investigated are shown in Fig. 3. Most of the samples have smooth and featureless surfaces, particularly the C-NiO based samples presented in Fig. 3 (a) and (b). Some C-NiO samples shown in Fig. 3 (b) had ‘dendritic’ features, the origin of which is not clear yet.

Analysis by EDS (not shown here for brevity) was done on the clear and on the ‘dendritic’ regions. No difference between the relative atomic compositions of carbon, nickel and oxygen in the two different regions was found, conceding that EDS would not give accurate quantitative measurements for light elements such as carbon and oxygen. All C-ZnO based samples represented

by Fig. 3 (c) show features of the substrate surface, such as striations scratch marks, perhaps indicating the transparent nature of ZnO.

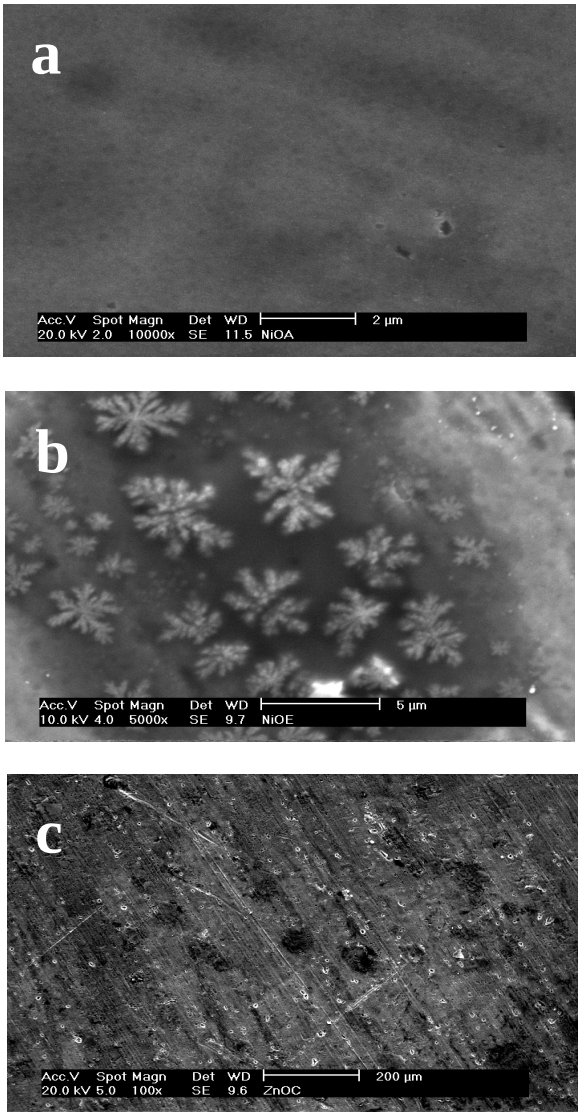

Fig. 3: SEM images of the different types of samples investigated (a) C-NiO, (b) C-NiO (dendrites) and (c) C-ZnO. All samples were deposited on aluminium substrates.

4.2 X-HRTEM, EDS and EELS results

The C-ZnO and C-NiO have been studied by cross-sectional transmission electron microscopy (TEM). The cross-sectional specimen was prepared on a focus-ion-beam (FIB) workstation.

The low magnification bright field image in Fig. 4 showed that the sol-gel C-NiO coating is nano-crystalline. It should be noted that there are disk-like pores with diameter of about 200 nm in the coating. A cross-sectional high resolution transmission electron microscope (X-HRTEM) image shown in Fig. 5 revealed that the nano-crystalline grains are NiO. The selected area electron diffraction (SAED) result shown in Fig. 6 also demonstrated that in most regions, the coating consisted of nano-crystalline NiO.

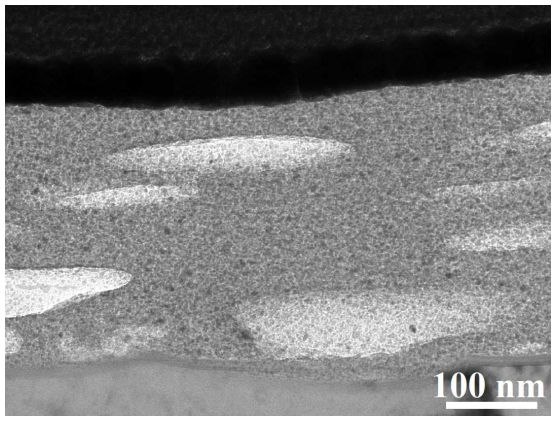

Fig. 4 A bright field image of C-NiO coating.

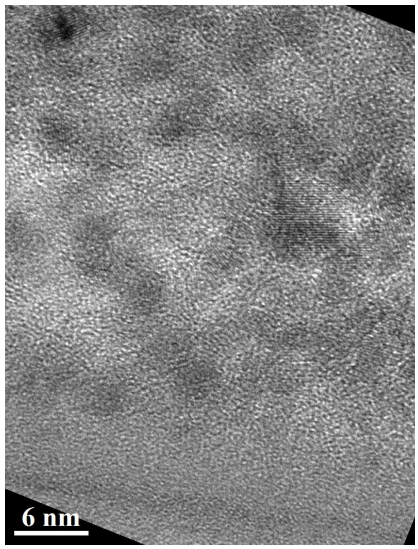

Fig. 5 A high resolution TEM image of C-NiO coating.

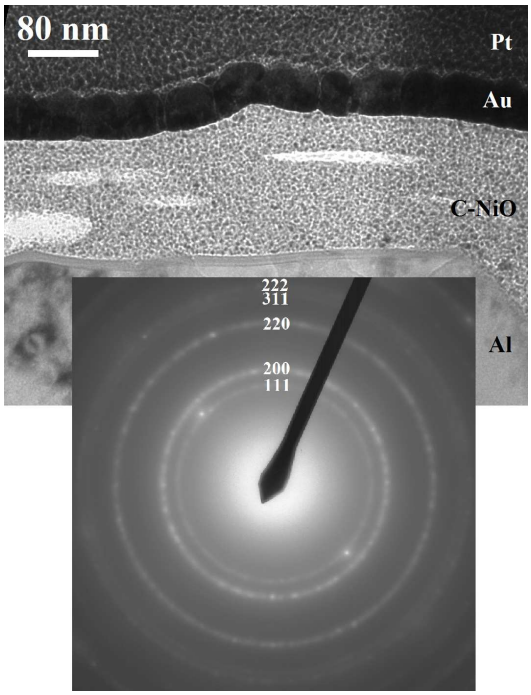

Fig. 6 A TEM image together with the corresponding selected area electron diffraction pattern of a C-NiO sample.

Chemical composition analysis both by EDS and EELS shows that the film contains carbon (see Fig. 7), but since no crystalline carbon or carbide was found, it is surmised that the film contains amorphous carbon. The EELS mapping formed by using the C K peak at 290 eV with an energy window width of 20 eV is shown in Fig. 8. The electron diffraction reveals that there exists a small amount of Ni grains with diameter of about 30 nm in some regions of the film (see Fig. 9).

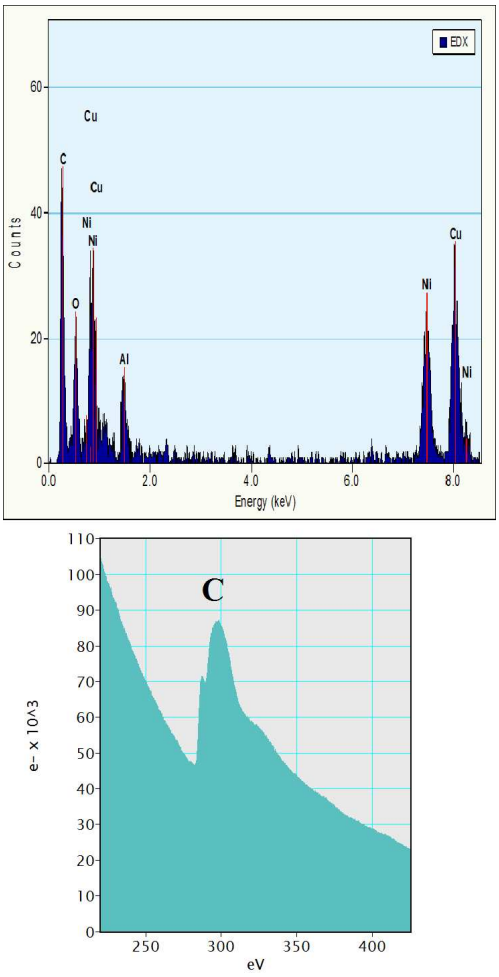

Fig. 7 EDS and EELS from the C-NiO coating. The Al and Cu signals are from the substrate and copper grid, respectively.

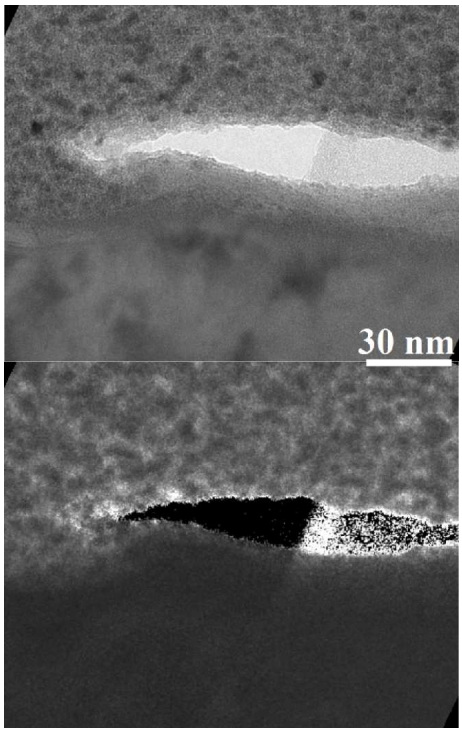

Fig. 8 (a) The zero loss image and (b) the corresponding EELS mapping of the C-NiO sample. The hole in the middle of the image is a pore in the composite coating.

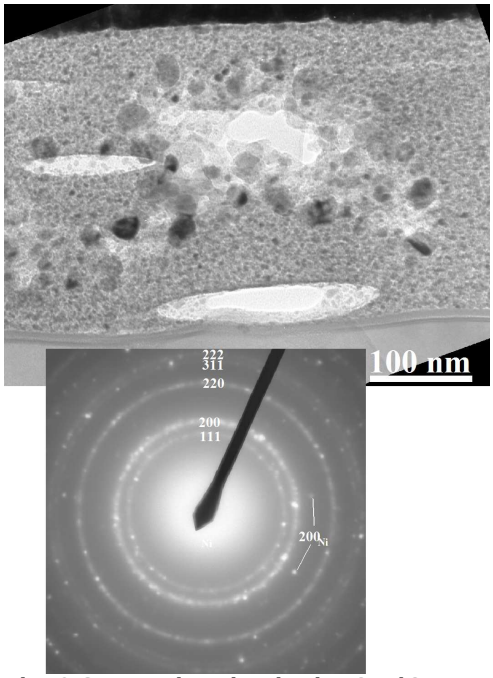

Fig. 9 Some Ni grains in the C-NiO sample. The inset is the corresponding SAED pattern.

4.3 XRD results

The results of the XRD experiments on some selected C-NiO and C-ZnO samples are shown in Fig. 10, together with the diffraction peaks of the aluminium substrate material. The majority of the C-NiO and C-ZnO samples investigated with the XRD technique indicate that both the carbon nanoparticles and the matrix materials are amorphous.

There were a few samples that showed some crystalline NiO and ZnO, with reflections (200) at 42.5° and (110) at 56.6° respectively, as indicated in Fig. 10. Similar observations have been made by Lee *et al.*(Lee, 2005) and by Hernandez and Mendoza-Galvin (Hernandez-Torres, 2005) for NiO. Jimenez-Gonzalez *et al.* (Jimenez-Gonzalez, 1998) and Liu *et al.* (Liu, 2005) made similar observations for ZnO. The absence of any carbon peaks in the diffraction patterns shown in Fig. 10 corroborates that the carbon nanoparticles are indeed amorphous. It is worth noting that EDS analysis as discussed earlier confirmed the presence of carbon, nickel, zinc and oxygen K-peaks.

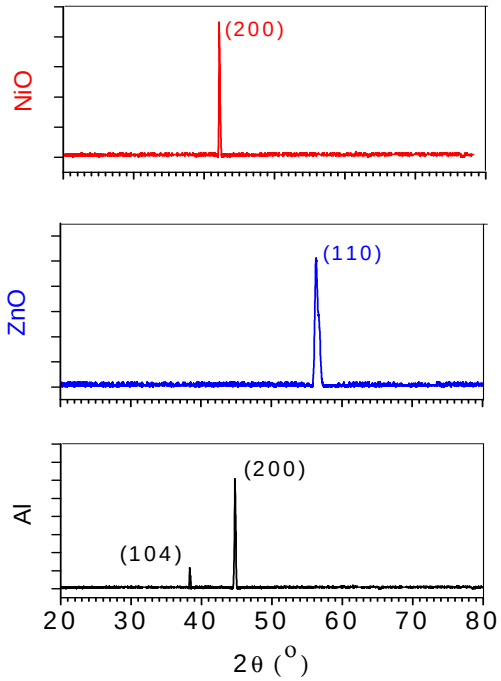

Fig. 10 The XRD pattern of selected C-ZnO and C-NiO samples. Some crystallites of the oxides are embedded in corresponding amorphous phases. The diffraction peaks for the aluminium substrate are included.

4.4 Near-normal solar absorptance and thermal emittance results

The reflectance spectra for C-ZnO and C-NiO samples are presented in Fig. 11 and Fig 12, respectively. An attempt has been made to check reproducibility of the samples of both types by maintaining the same deposition parameters. From TEM images (not shown), it was observed that the thickness range of the samples investigated here was between 0.8 µm to 1.0 µm. The spectra in both figures show that both types of samples have reasonable reproducibility.

In Fig 11, the dips in the spectra between 6 and 7 µm are due to water absorption (O-H bending vibrations at 1600 cm^{-1}) (Katumba, 2005; Rao, 2003). The O-H bending vibrations are much weaker than the case for previously studied C-SiO_2 samples (Katumba, 2005). This implies a lower emittance for the C-ZnO samples. The O-H stretching vibrations around 2.7 and 3.3 µm (3000 to 3600 cm^{-1}) of the C-SiO_2 samples are conspicuous by their absence in the ZnO system resulting in an even lower emittance.

The absorption due to the Zn-O vibrations is expected between 20 and 25 µm (Du, 2006; Matsumura, 2005), which is just beyond the measurement range for the present work. A major difference between these spectra and those of previous experiments on C-SiO_2 selective absorbers (Katumba, 2005) is the absence of strong absorption between 2.5 to 20 µm. This signifies a great improvement in emittance characteristics of the C-ZnO absorber coatings compared with those of the previous study of C-SiO_2 selective absorbers. Another added advantage is that the UV-VIS absorption of the C-ZnO-based samples seems somewhat better than those of C-SiO_2. However, a drawback of the C-ZnO-based absorber surfaces is that the transition step from low to high reflectance is not steep enough for all samples investigated.

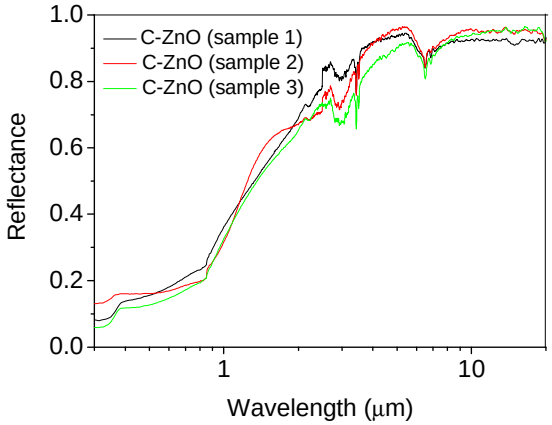

Fig. 11 The near normal reflectance spectra of C-ZnO samples of similar thicknesses showing a not-so-steep transition from low to high reflectance at about 2.5 µm.

The reflectance spectra of similar thicknesses of C-NiO samples are presented in Fig. 12. It is clear that both modes of the O-H vibrations of the ZnO samples are absent in the NiO. This yields even better emittance characteristics. The step transition for all the samples is between 2 and 3 µm and is steeper than that of the C-ZnO samples. The absorption can be further enhanced by applying an antireflection (AR) coating, which minimally affects the emittance as has been demonstrated by Boström *et al.* (Boström, 2004).

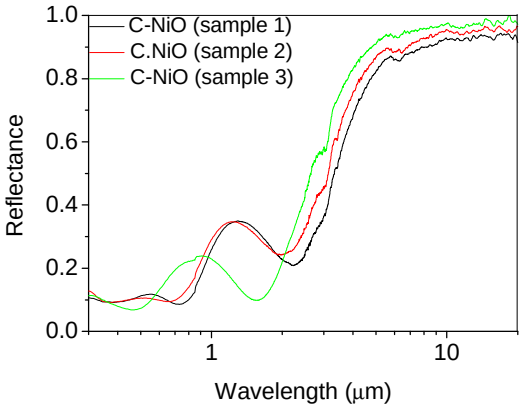

Fig. 12 The near normal reflectance spectra of NiO samples of similar thicknesses showing a steep transition from low to high reflectance at about 2.5 µm.

A qualitative comparison of the two types of samples used in this work is made in Fig. 13 for samples of similar coating thicknesses. It is evident that the C-NiO samples exhibit the better behaviour expected of a selective solar absorber than the C-ZnO samples. Fig. 13 also includes the reflectance spectrum of a coating of commercial grade solkote paint on an aluminium substrate made by a spray-painting technique. Solkote paint is used here for comparison because the sols used in the experiments reported here have similar formulation principles as the paint.

The Solkote paint sample exhibits superior absorption characteristics compared to the other samples, but it nevertheless has inferior emittance characteristics compared to the C-ZnO and C-NiO samples. A quantitative comparison of all the samples is presented in Table 1. A figure of merit calculated as α/ε indicates that the C-NiO samples are superior to both the C-ZnO and the solkote paint samples in solar absorber selectivity behaviour.

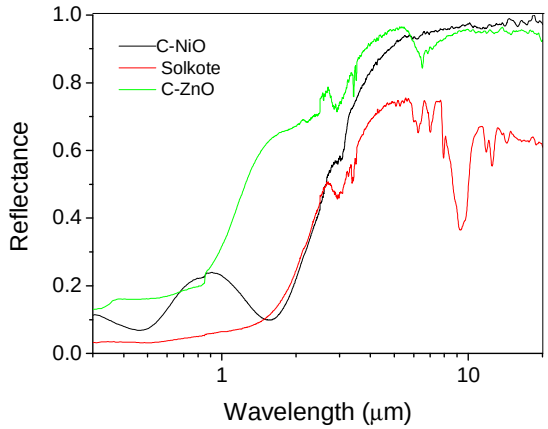

Fig. 13 The solar selectivity curves of C-ZnO and C-NiO based samples. The curve for a commercial Solkote paint is included for comparison.

Sample	α	ε	α/ε
Solkote	0.93	0.33	2.85
C-ZnO	0.71	0.06	12.70
C-NiO	0.84	0.04	20.91

Table 1: The solar selectivity of the C-ZnO, C-NiO and solkote paint coatings on aluminium substrates. A figure of merit is given in column 4 for easier comparison

Fig. 14 summarises the most important results obtained in this experiment in the form of a quadrant plot. It shows the NiO based samples perform better than the ZnO based samples. The data points falling in quadrant I have the best selectivity characteristics while those in quadrant III have the worst selectivity characteristics. The data points in quadrants II and IV are for samples that may need slight change in one or two of the various fabrication parameters so that they could then qualify to be in quadrant I. The quadrants were formed from a rule of thumb that a good selective absorber should have a solar absorptance of at least 80% and a thermal emittance of less than 20%.

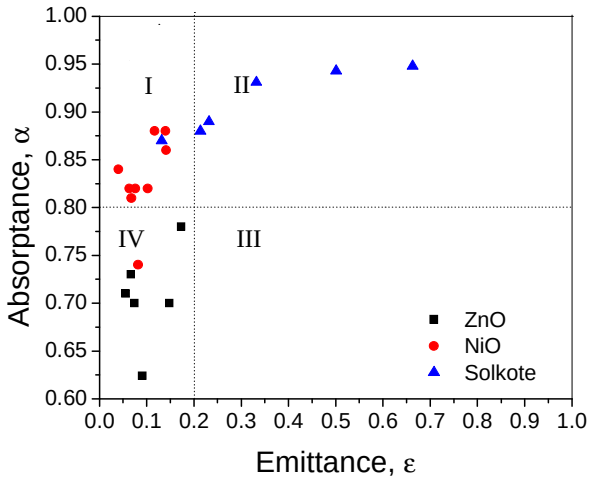

Fig. 14 Graph showing that C-NiO samples have the best solar selectivity compared with C-ZnO and commercial solkote paint samples. Each data point refers to a tested sample.

5. Conclusions

This work has demonstrated that it is possible to prepare tandem solar selective absorber surfaces with carbon nanoparticles embedded in oxide matrices of zinc or nickel on aluminium substrates. The normal thermal emittances of the samples were 6% for the C-ZnO and 4% for the C-NiO samples. The normal solar absorptances were 71% and 84% for ZnO and NiO samples, respectively. The C-NiO based absorber surface therefore exhibited better solar selectivity behaviour than the C-ZnO. The C-NiO based absorbers also excelled the solar selectivity of commercial Solkote paint coatings on aluminium. Thus C-NiO selective

surfaces could be used in the construction of low cost selective solar absorbers in rural Africa as well as peri-urban settlements.

We propose to make the leap from laboratory concept to a working prototype, with the aim to produce selective solar absorbers for low cost domestic heating in rural areas. This involves applied research into adapting the fabrication process to allow for large surface area prototype development, and the testing of the prototype by using dedicated solar collection panels. Some structural analysis of the samples have been made to understand the optical and thermal behaviour of the coatings, but accelerated ageing tests are needed to gain knowledge about the durability of the coatings in real-life application environments. Finally, there is a consortium interested in doing real-life testing of the final devices in rural areas for low cost domestic heating, such as heating and boiling water, and cooking food.

This technology would have a material impact on the lives of the poorest people in South Africa by providing them with a reliable energy source for domestic heating applications. This is precisely the mandate of the CSIR. One cannot over estimate the impact of such a device. For example, to give the ability to boil water to a rural household without the need for electricity or making a flame would have a huge impact on their safety, health and would generally result in a better quality of life for such communities.

Acknowledgements
The University of Zimbabwe, Harare, and the Uppsala University, Sweden, through SIDA/SAREC provided research grants for the work reported here.

References

Avila-Garcia, A. and Morales-Ortiz, U., 2006. Solar Energy Materials & Solar Cells: 90: 2556–2568.

Boström, T.K., Wäckelgård, E. and Westin, G., 2004. Solar Energy Materials & Solar Cells: 84: 183–191.

Du, X-W., Fu, Y-S., Sun, J., Han, X. and Liu, J., 2006. Semicond. Sci.: 21: 1202–1206.

Hernandez-Torres, J. and Mendoza-Galvin, A., 2005. Journal of Non-Crystalline Solids: 351: 2029–2035.

Jimenez-Gonzalez, A.E., Urueta, J.A.S. and Suarez-Parra, R., 1998. Journal of Crystal Growth: 192: 430–438.

Katumba, G., Forbes, A., Olumekor, L. and Makiwa, G, 2008a. Proc. SPIE, 7046: 70460B1-8.

Katumba, G., Olumekor, L., Forbes, A., Makiwa, G., Mwakikunga, B, Lu, L. and Wackelgard, E., 2008b. Solar Energy Materials & Solar Cells, 92: 1285-1292.

Katumba, G, Mwakikunga, B.W. and Mothibinyane, T.R., 2008c. Nanoscale Research Letters, 3: 421-426.

Katumba, G., Lu, J., Olumekor, L., Westin, G. and Wäckelgård, E., 2005. J. Sol-Gel Science and Technology: 36: 33–43.

Konttinen, P., Lund, P.D. and Kilpi, R.J., 2003. Solar Energy Materials & Solar Cells: 79: 273–283.

Lee, J.Y., Liang, K., An, K.H. and Lee, Y.H., 2005. Synthetic metals: 150: 153–157.

Liu, Z., Jin, Z., Li, W. and Qui, J., 2005. Materials Letters: 59: 3620–3625.

Makiwa, G, Katumba, G. and Olumekor, L., 2008. Proc. SPIE, 7046: 70460A1-8.

Matsumura, M., Bandic, Z. and Camata, R.P., 2005. Mater. Res. Soc. Symp. Proc. 869: D1.7.1–D1.7.6.

Niklasson, G.A and Granqvist, C.-G., 1984. J. Appl. Phys.: 55: 3382–3410.

Orel, Z.C., 1999. Solar Energy Materials & Solar Cells: 57: 291–301.

Rao, A.V., Kalesh, R.R. and Pajonk, G.M., 2003. J. Mater. Sci.: 38: 4407–4413.

Wäckelgård, E., Niklasson, G.A. and Granqvist, C.G., 2001. Chapter 3: Selectively solar-absorbing coatings, in Energy-The State of the Art (James and James Science Publishers Ltd. London).

Zhao, S. and Wäckelgård, E., 2006. Solar Energy Materials & Solar Cells: 90: 243–261.